# Development of Single-Cell Live Sorting Platform - Nanowell-LIFT

Yuntong Wang[a,b], Ying Xue[e], Xi Hong[e], Huan Wang[a], ChunYang Zhou[f], Wei Wang[g,h,i], Peng Liang[a,e], Hang Li[e], Qingmei Xu[g,h,i], Yu Wang[a,b], KunXiang Liu[a,b], LinDong Shang[a,b], Hao Peng[a,b], Fuyuan Chen[a,b], Huabing Yin[j], Yun Wang[c], Wei E. Huang[c,d,*], Bei Li[a,e,*]

[a]Changchun Institute of Optics, Fine Mechanics and Physics, Chinese Academy of Sciences, Changchun 130033, P. R. China

[b]University of Chinese Academy of Sciences, Beijing 100049, P. R. China

[c]Oxford Suzhou Centre for Advanced Research (OSCAR), University of Oxford, Suzhou Industrial Park, Jiangsu, P.R. China.

[d]Department of Engineering Science, University of Oxford, Parks Road, Oxford, OX1 3PJ, United Kingdom

[e]Hooke Laboratory, Changchun 130033, P. R. China

[f]Biomedical Engineering, School of Life Science and Technology, Changchun University of Science and Technology, Changchun, 130031, China

[g]School of Integrated Circuits, Peking University, Beijing, China

[h]National Key Lab of Micro/Nano Fabrication Technology, Beijing, China

[i]Beijing Advanced Innovation Center for Integrated Circuits, Beijing, China

[j]James Watt School of Engineering, University of Glasgow, Glasgow, U.K.

*Corresponding author:

Wei E. Huang and Bei Li

Tel: 01865 283786 and 0431-86708966

Email: wei.huang@eng.ox.ac.uk and beili@ciomp.ac.cn

## Table of Contents (TOC)

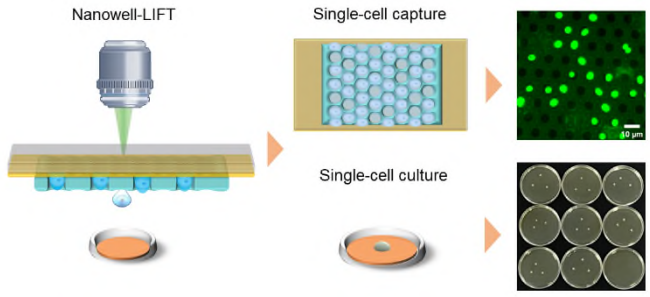

**ABSTRACT**

Single-cell research provides a compelling approach for understanding life's intricacies at the most fundamental level, offering a high-resolution lens for studying cell biology. Laser-induced forward transfer (LIFT) technology is a simple method to accurately isolate individual cells, but it still faces challenges such as low throughput of single-cell capture efficiency and cell damage. To address these challenges, we have developed an automated platform called Nanowell-LIFT. This innovative system facilitates single-cell sorting from culture medium or liquid solution, utilizing a nanowell ejection chip (N-chip). Our Nanowell-LIFT has been applied successfully to achieve enhanced efficiency and throughput for live cell capture and isolation, with applications spanning microorganisms *Escherichia coli*, *Saccharomyces cerevisiae*, *Cyanobacteria* spp., and *Chlamydomonas* spp. This innovative tool overcomes the liquid's surface tension and reduces the required laser energy thus achieving accurate live cell sorting. The Nanowell-LIFT platform exhibits a good performance: above 80% single-cell capture efficiency, nearly 100% sorting efficiency, over 95% cell viability, 100% sorting accuracy (confirmed by sequencing), and over 88% genome coverage of single cells, which represent a prominent leap forward in LIFT technology compared to traditional methods. These results not only illustrate the potential of the Nanowell-LIFT platform but also set the stage for broader applications of single-cell research, heralding new possibilities in the understanding and manipulation of life at its most fundamental level.

**KEYWORDS:** single-cell capture, single-cell live sorting, laser-induced forward transfer, nanowell ejection chip, Nanowell-LIFT, temperature simulation.

Single-cell research has risen to prominence as a potent tool for unravelling the intricacies of biological systems. Traditional methodologies, which rely on average measurements across cell populations, have often concealed the inherent heterogeneity in cell types. This obscurity constrains our comprehension of genetic, epigenetic, and proteomic variances amongst cells.[1] Currently, single-cell research has already contributed to many important discoveries in various fields, including early embryonic development,[2, 3] tumor heterogeneity,[4-6] and microbial diversity,[7-9] and is exceedingly needed in rare samples, such as circulating tumor cells,[10, 11] immune cells in autoimmune diseases,[12, 13] and human gut microbiome.[14, 15] In addition, since most bacteria in nature are not cultured yet, the study cells at the single cell level would shine a light of functionality in microbial ecology.[16] However, single-cell sorting, which serves as the foundation for single-cell research, continues to present formidable technical challenges.

The urgent need to sort the single cells based on differences in single-cell heterogeneity information has motivated many approaches, such as fluorescence-activated cell sorting (FACS),[17] magnet-activated cell sorting (MACS),[18, 19] laser capture microdissection (LCM),[20, 21] optical tweezer (OT),[22, 23] limiting dilution,[24, 25] manual micromanipulation,[26] acoustic droplet ejection (ADE),[27, 28] and laser-induced forward transfer (LIFT).[29, 30] However, FACS and MACS are limited to labeling with either fluorescent stains or magnetic microbeads. They are limited to sorting cells with fluorescent markers. LCM is complex to operate and uses a high-power UV laser, which has an adverse impact on cell viability. OT is only suitable for screening cells suspended in a transparent liquid environment and needs tedious sample collection steps. Limiting dilution and manual micromanipulation are inefficient for sorting single cells. ADE is unable to capture individual cells in the source fluid wells, and the limited target volume of droplet coalescence prevents it from accurately sorting individual tiny microbial cells.

In contrast, LIFT technology has significant advantages including label-free, automated, and precise sorting of individual cells, easy to collect, no requirement for sample transparency, and the ability to sort multi-sized microbial cells (1-30 μm) or irregularly shaped cells.[31-35] The pulsed laser produces a microburst that acts as a driving force to eject the target sample toward the receiving substrate by utilizing the interaction between the laser and material. However, sorting dried samples using LIFT offers advantages such as easy positioning and prevention of sample drift, but it is prone to sample aggregation, which results in low single-

cell capture rate and poor cell viability. On the other hand, liquid sample sorting by LIFT can enhance cell viability, but precise positioning and single-cell capture are unable to be achieved. Additionally, the high laser energy required in liquid sorting can cause cell damage as it not only overcomes the surface tension of the liquid, but also drives sample separation. During the process, the sorting pressure is lower than the pressure that cells can tolerate, and thermal interference generated by laser ablation of materials can cause substantial damage. The low viability of single cells greatly affects the significance of single-cell research. Single-cell capture[36, 37] and cell damage[38-40] remain significant obstacles for efficient single-cell sorting by conventional LIFT.

Here we develop an automated platform for single-cell ejection sorting that uses a wettability-based nanowell ejection chip (N-chip) in combination with LIFT technology (Nanowell-LIFT). The wettability-based nanowell ejection chip overcomes the liquid's surface tension, thereby reducing the energy required for LIFT sorting, minimizing cell damage, and preserving cell viability. We demonstrate that Nanowell-LIFT is able to capture and sort single cells of various microorganisms such as *Escherichia coli*, *Saccharomyces cerevisiae*, *Cyanobacteria* spp., and *Chlamydomonas* spp.. Nanowell-LIFT system would provide an efficient and robust method for single-cell capture and sorting. This approach holds great promise for broader applications of single-cell research.

## RESULTS AND DISCUSSION

### Nanowell-LIFT: Design and Operating Principle

A Nanowell-LIFT platform was developed to address the limitations of existing methods by using an N-chip (Figure 1a). The Nanowell-LIFT platform comprises the following components: an ejection sorting system, an imaging recognition system, a 3D mobile system, a receiving system, and an N-chip (Figure S1). The N-chip (Figure S2a) includes a glass plate, a hydrophilic sacrificial layer (Figure S2b), and a hydrophobic nanowell array film (Figure S2c).[41] About 400,000 geometrical nanowell units were innovatively designed using wettability-based hydrodynamic traps, which can efficiently capture individual cells. When the cells are loaded onto the nanowell ejection chip, the hydrophilic bottom layer and the hydrophobic wall of the nanowell created a trap to capture hydrophilic cells into the nanowells. This design nanowell

enables individual cells from the suspension to set into nanowells. After cell loading, we can perform automated detection, capture, identification, and ejection (Figure 1b-e and Movie S1). The principle of the nanowell structure combines hydrokinetics with surface wettability, differing from the single-cell sorting method of conventional LIFT technology on metal-coated ejection chips. In conventional metal-coated ejection chips, the thickness of the liquid layer (D1: 30-100 μm) is not immobilized, resulting in lateral migration of cells that hinders the capture of individual cells. Moreover, the formation of jets during the sorting process leads to multiple cells being sorted together. This process requires overcoming the surface tension of the liquid and driving sample separation, which necessitates higher laser energy that can easily cause cell damage (Figure 1f, g). In contrast, the Nanowell-LIFT method utilizes N-chips, which disperse the suspension liquid containing target cells into individual droplets, achieving single-cell capture. Unlike conventional metal-coated ejection chips, there is no need to overcome the liquid's surface tension; only driving sample separation is necessary. As a result, less laser energy is required, leading to a significant reduction of cell damage (Figure 1h, i). The Nanowell-LIFT method proves to be an excellent approach for capturing and sorting single cells.

**N-chip: Precise Fabrication and Pre-treatment**

The N-chip represents a novel ejection sorting tool, combining the conventional metal-coated ejection chip[29, 30, 42] with a nanowell array film. To fabricate the nanowell array films, we utilized a combination of Si master lithography, chemical vapor deposition (CVD), reactive ion etching (RIE), HNA (HF: $HNO_3$: HAc = 5:7:11, v/v) release techniques (Figure 2a-d). We successfully produced films with varying hexagonal outer circle diameters, including 8 μm, 10 μm, and 15 μm (Figure 2e and Figure S3). To assemble the N-chip, a 25-nm aluminum metal film was evaporated on a glass plate (Figure 2f), followed by plasma treatment of the metal-coated glass and the nanowell array film (Figure 2g). The plasma-treated surfaces we developed were subsequently integrated to create the N-chip (as illustrated in Figure 2h), which is designed specifically for the capture and sorting of single cells.

**Characterization of the Performance of the Single-Cell Capture for N-chips**

In this study, we imaged and observed *Saccharomyces cerevisiae* (*S. cerevisiae*) cells captured by the conventional metal-coated ejection chip and the N-chip. Figure 3a and b

revealed that the traditional chip failed to capture *S. cerevisiae* cells due to the unfixed thicker liquid layer, which caused the lateral migration of cells to aggregate into a ring. In contrast, the N-chip successfully dispersed the cells into single-cell microdroplets and achieved efficient single-cell loading in the N-chip. To calculate the capture efficiency of the N-chip, we counted single *S. cerevisiae* cells (below 5 μm) captured in each nanowell structure (8 μm). The evaluation of single-cell capture efficiency was conducted by calculating the ratio of individual cells captured to the total number of cells collected within the nanowell. The degree of single-cell capture efficiency was directly linked to the subsequent success of the single-cell sorting process. According to our findings, the capture efficiency increased when lower concentrations of microbial concentrations were used (Figure 3e). The single-cell capture efficiency reached nearly 100% when the cell suspension concentration was at $10^5$ - $10^6$ cells/ml. This was verified through six independent experiments. However, the nanowell use efficiency is low (Figure S4a, b). We then measured the single-cell capture efficiency for other cell suspension concentrations: 96.77% was observed for $10^7$ cells/ml, 90.64% for $5\times10^7$ cells/ml, and 63% for $10^8$ cells/ml. The cells captured at these three concentrations are shown in Figure 3c, h, and d. These results suggest that the cell suspension concentration of $5\times10^7$ cells/ml can yield high capture efficiency and a good nanowell use efficiency. Hence, we used $5\times10^7$ cells/ml as the loading concentration in later experiments.

We also quantified the capture efficiency using nanowells of different pore sizes (8 μm, 10 μm, and 15 μm) for various microorganisms, including *Escherichia coli*, *S. cerevisiae*, *Cyanobacteria* spp., and *Chlamydomonas* spp. Figure 3f shows the mean and median of single-cell capture efficiency at different parallel experiment counts. These cells captured by nanowells with other pore sizes under $5\times10^7$ cells/ml suspension concentrations were shown in Figure S4c-j. According to the results, 8 μm pore size of nanowell can achieve the best single-cell capture efficiency, which were 90.32% for *Escherichia coli* (*E.coli*), 90.64% for *S. cerevisiae*, 82.55% for *Cyanobacteria* spp., and 81.98% for *Chlamydomonas* spp. (Figure 3g–j). Attaining high single-cell capture efficiency lays a crucial foundation for the ensuing processes of cell sorting and collection.

**Nanowell-LIFT Provides Efficient Single-Cell Sorting Performance**

To assess the single-cell sorting capability of the Nanowell-LIFT platform, we orchestrated a

set of experiments to gauge the single-cell sorting efficiency across a range of microorganisms. This was achieved by fine-tuning the laser energy (as illustrated in Figure 4a). Each level of laser energy was put to the test twenty times across different cell lines. The single-cell sorting efficiency was then determined by quantifying the ratio of successful single-cell sorting instances to the total number of sorting attempts. Our findings unambiguously established that the single-cell sorting efficiency across various cell lines amplified in tandem with increasing laser energy. As shown in Figure 4a, the 120 nJ laser energy was found the optimal condition for single-cell sorting. Based on this finding, we successfully conducted experiments utilizing the Nanowell-LIFT system to sort individual *S. cerevisiae* cells with a laser energy of 120 nJ and a 0.17 mm thick cover glass as a receiver for imaging the sorted cells (Figure 4b). As shown in Figure 4b, we reduced the imaging interference of water droplets on the glass cover. This process showed the successful identification of a single target cell, the ease of one-click laser sorting, *in situ* verification post-sorting, and confirmation of an *S. cerevisiae* cell through bright-field and fluorescence imaging observations of the receiver before and after sorting. Conversely, liquid sorting experiments involving *S. cerevisiae* using the traditional LIFT system, even at a peak laser energy of 11 μJ posed significant challenges. These were largely attributed to the lateral migration of cells in the thicker liquid layer and the greater surface tension of the liquid, both of which complicated the capture and sorting of individual cells. Even though the sacrificial layer was successfully ablated by the laser, the cells were not effectively sorted (as depicted in Movie S2). In contrast, the Nanowell-LIFT platform demonstrates good stability and efficiency in single-cell sorting, thereby proving its suitability for sequential automation control.

**Simulation of Effects of Temperature on Cell Sorting Performance**

To evaluate possible damage to cells during the cell sorting process, we conducted simulations of the temperature changes induced by 5 ns pulsed laser ejection. To achieve this, we set the conditions for single-cell sorting, including a laser energy of 120 nJ, a nanowell pore size of 8 μm, a nanowell depth of 10 μm, and an Al-coating thickness of 25 nm. It is shown that the temperature variation of the sacrificial layer due to laser ablation followed a Gaussian distribution and propagated into the liquid over time (Figure 4c-e and Figure S5). To quantify the process, we calculated and plotted the temperature model as a function of the vertical

distance and time of the laser action (Figure 4f). Notably, the Royal Blue area remained continuously below 30 degrees Celsius, suitable to live cell sorting. The results also indicate the position 2.5 μm from the sacrificial layer surface was always maintained below 30 degrees Celsius, remarkably lower than the 2100 degrees Celsius on the Al-sacrificial layer surface (Figure 4g, h). We specifically targeted microbial cells smaller than 5 μm, positioned well over 2.5 μm away from the sacrificial layer surface within a nanowell of 10 μm height, owing to the force of gravity when the chip was inverted. Thus, the temperature generated by 120 nJ laser energy did not affect cells located further than 2.5 μm away from the sacrificial layer surface. In contrast, the traditional LIFT system was unable to achieve single-cell sorting, even when utilizing 11 μJ laser energy. This was primarily due to the lateral migration of cells within the denser liquid layer and the increased surface tension of the liquid, both of which inhibited the successful capture and sorting of individual cells. A simulation of this process revealed that heat rapidly diffused into a 10 μm thick liquid domain, with the maximum temperature reaching up to $10^5$ degrees Celsius. This is far beyond the survival threshold for microorganisms (as displayed in Figure S6a-c). Remarkably, the sorting energy required for the Nanowell-LIFT platform was only 120 nJ, which is significantly less than the energy required for conventional LIFT ejection sorting.

To further investigate the temperature distribution, we also simulated the temperature diffusion of N-chips with nanowell pore sizes of 10 μm and 15 μm (Figure S6d, e). As the nanowell pore size of the N-chip increased, the temperature diffusion range decreased, and the Royal Blue area (representing temperatures below 30 degrees Celsius) increased in Figure S6f, g. These results excluded the possibility of damage caused by laser ejection with N-chips and ensured that cell viability was not affected.

**Verification of cell viability using Nanowell-LIFT**

To verify the efficacy of the Nanowell-LIFT system, we conducted two sets of experiments to confirm the viability of single-cell sorting. We sorted live cells of 72 *E. coli* and 72 *S. cerevisiae* at the single-cell level. Each receiver was sorted three times so that each receiver might get three microbial cells. There were eight parallel groups and one negative control group. All experiments were repeated three times to ensure accuracy and reliability (Figure 5a). The survival rate of single-cell sorting by the Nanowell-LIFT system was 97.2% for *E.coli* cells and

95.8% for *S. cerevisiae* cells, which was higher than the conventional LIFT (Figure 5b).[40] To further confirm the sorted cells, rRNA was amplified and sequenced by picking clones from each of the eight dishes containing the sorted cells. The positive bands were produced from 9 clones of the sorted *E. coli* using the 27F/1492R primer pair for 16S rRNA analysis (Figure 5c). Similarly, for 9 clones of the sorted *S. cerevisiae*, positive bands were generated using the NL1/NL4 primer set for LSU rRNA analysis (Figure 5d). The sequence alignments were 100%, confirming the sorted cells were targeted *E. coli* and *S. cerevisiae* (Figure S7).

**Genome sequencing for single cells sorted by Nanowell-LIFT**

We carried out genome resequencing on individual *E. coli* cells sorted using both the Nanowell-LIFT and conventional LIFT systems. This process involved sorting and analysing five separate cells. Our results demonstrated that the base coverage for single cells achieved via the Nanowell-LIFT system significantly outstripped that provided by the conventional LIFT system, given an equal number of genome bases. As detailed in Table 1, we recorded genome coverage at 88% for Nanowell-LIFT, as opposed to 38% for the conventional LIFT system. Hence, the Nanowell-LIFT platform is an excellent strategy for single-cell cultivation and genomic analysis.

## CONCLUSIONS

Selective single-cell sorting is essential in a multitude of biomedical applications. Current methods for cell isolation face challenges such as sorting only labeled cells of the same species, limited sample number and status, complex operation, inefficient sorting, and tedious sample collection steps. The LIFT technology can overcome the above problems, but is limited to low single-cell capture efficiency poor success rate of single-cell sorting,[36, 37] enormous cell damage, and low genome coverage.[38-40] In contrast, the Nanowell-LIFT system developed in this study does not need to overcome the surface tension of the liquid but only to drive the sample separation, thus requires less laser energy and significantly reduces cell damage, which offers many advantages in terms of (i) high-efficiency single-cell capture (capture efficiency of above 80%), (ii) achieving stable and continuous automated single-cell visual sorting (nearly 100% sorting efficiency by 120 nJ laser energy), (iii) sorting without heat

damage, and (iv) over 95% cell viability, 100% sorting accuracy (confirmed by sequencing), and over 88% genome coverage. These improvements facilitate a significant leap forward in LIFT technology compared to traditional methods. These outstanding performances indicate that our system has enormous potential in single-cell research.

Single-cell capture efficiency is a vital parameter for obtaining enough single cells to perform downstream experiments. A meticulous assessment of all parameters influencing single-cell capture efficiency is necessary for successful subsequent operations. The Nanowell-LIFT system cuts suspension liquid dispersed by the target cells into individual droplets by the N-chips, achieving efficient single-cell capture of different cell lines. The Nanowell-LIFT system addresses the issues of the conventional LIFT system, in which the liquid layer is unstable, lateral migration of cells prevents the capture of individual cells, and multiple cells are sorted together during subsequent sorting processes.[36, 37] Overall, our findings can help extend single-cell heterogeneity study to a broad range of research areas by optimizing single-cell capture efficiency.

Cell damage is another crucial factor to consider in single-cell sorting processes. To maximize cell viability, we must complete single-cell sorting in a liquid environment and achieve 100% single-cell sorting efficiency with minimal energy. The Nanowell-LIFT system utilizes the N-chips to break the surface tension of the liquid enabling sample separation with minimal energy consumption, lowering the energy threshold of the LIFT, reducing cell damage, and maintaining cell viability. Experimental results showed that the survival rate of single-cell culture was 97.2% for *E. coli* cells and 95.8% for *S. cerevisiae* cells, and the single-cell genome coverage for *E. coli* was 88%. These results further confirm the validity of simulations and demonstrate that the Nanowell-LIFT system outperforms conventional LIFT in terms of single-cell viability and efficiency.[38-40]

The Nanowell-LIFT system is a breakthrough in single-cell sorting that addresses the limitations of conventional LIFT technology.[36-40] The system has been designed to achieve stable and efficient single-cell capture, as well as accurate and low-damage single-cell sorting. These advantages make it an ideal platform for various biological sciences and clinical research applications. As such, we anticipate that our system will be of significant value for single-cell heterogeneity research and analysis, paving the way for novel discoveries and

breakthroughs for microbial community study.

## METHODS

### System Setup

The all-in-one Nanowell-LIFT automated platform included a single-cell sorting module, a brightfield (fluorescent) imaging module, a 3D mobile stage, a receiver, and an N-chip. The single-cell sorting module consisted of a 532-nm laser pulse with 5ns full-width half-maximum (FWHM) duration (CNI Co. Ltd., China), a half-wave plate, a polarization beam splitter, and a beam expander (Lens 1, focal length f = 15 mm; Lens 2, focal length f = 50 mm), mirrors and a microscope objective (Nikon, 10x). The imaging module included a microscope objective (Nikon, 50x), mirrors, a beam splitter (a dichroic mirror, an exciting filter, and an emitting filter), a LED, and a camera (Do3think Co. Ltd., China). The N-chip was placed on the 3D mobile stage (JC Co. Ltd., China). The receiver was placed inside a 24-hole turntable, moved by electric control. Unless otherwise specified, Optical elements were purchased from Thorlabs.

### Nanowell Design and Fabrication

The hydrophobic nanowell array film was meticulously fabricated at the Peking University Microelectronics Technology Cleanroom Facility. The process began with a four-inch silicon master plate, on which the photoresist was spun coated for photolithography. This step resulted in a hexagonal microcolumn template with a height of 10 μm. Subsequently, a Parylene C layer was applied using a commercial Parylene deposition instrument via chemical vapor deposition (CVD). Reactive ion etching (RIE) of the deposited Parylene C layer was performed to expose the top of the silicon pillars. Finally, the nanowell Parylene C membrane was released from the Si master by immersing it in HNA. The delicate fabrication process ensures the precise formation of the hydrophobic nanowells (10mm*10mm), thereby allowing for highly efficient and reliable single-cell capture and sorting.

### Cell Culture

A commonly used medium for cultivating *S. cerevisiae* is YPD, which consists of yeast extract, peptone, and dextrose. The optimal temperature for the growth of *S. cerevisiae* is 30 °C, and the optimal pH range is 4-6. *E. coli* is cultivated in LB (Luria-Bertani) broth, which includes

tryptone, yeast extract, and NaCl. The optimal temperature for the growth of *E. coli* is 37 °C, and the optimal pH range is 6.5-7.5. For *Cyanobacteria* spp., BG-11 medium is commonly used, containing $NaNO_3$, $K_2HPO_4$, $MgSO_4$, $CaCl_2$, $Na_2CO_3$, and trace elements. The optimal temperature for the growth of *Cyanobacteria* spp. is 25-30 °C, and the optimal pH range is 7.5-9.5. the cultivation of *Chlamydomonas* spp. can be cultivated using Tris-acetate-phosphate (TAP) medium, which consists of $NH_4Cl$, $MgSO_4$, $CaCl_2$, $KH_2PO_4$, and trace elements. The optimal temperature for the growth of *Chlamydomonas* spp. is 25 °C, and the optimal pH range is 7.0-7.5.

**Capture Characterization and Optimization**

An orthogonality experiment with various *S. cerevisiae* cell concentrations ($10^5$, $10^6$, $10^7$, $5\times10^7$, and $10^8$ cells /ml) and 8 μm pore size as the primary influencing factors were set to optimize the capture efficiency at the highest concentration. Additional cell lines (*E. coli* cells, *S. cerevisiae* cells, *Cyanobacteria* spp., and *Chlamydomonas* spp.) were captured using different pore sizes (8 μm, 10 μm, and 15 μm) at optimal concentrations ($5\times10^7$ cells /ml), showed a significant effect on capture efficiency. All cell solutions have fully oscillated before each test for single-cell capture efficiency.

**Automated Single-Cell Isolation**

Before the sorting experiment, the Nanowell-LIFT device and the N-chip were exposed to UV light for at least 30 minutes to eliminate other bacterial contamination. After that, the metal-coated glass and the nanowell array film were processed using $O_2$ plasma under controlled conditions of 200 W, 400 sccm, and 1.5 min. Next, a precisely measured 2 μl cell suspension volume was meticulously added to the treated N-chip for single-cell capture, completed in approximately 15 seconds. Subsequently, the chip was placed on a 3D motion platform, and a CCD camera recorded all of the isolation and collection procedures interfaced with a computer. The entire sorting process was expertly controlled using a single click, which resulted in the precise sorting of target cells into the designated receiver or the corresponding culture medium, per the experimental protocol.

**Simulation of Single-Cell Sorting Processes**

The simulation of the single-cell sorting process involved a physical model, which was implemented in the Heat Transfer Module from COMSOL Multiphysics. In this model, the laser

beam acted on a metal film, generating heat energy that caused the surrounding liquid to heat up. The laser beam was modeled as a heat source over a physical domain consisting of metal material to simulate this process. The temperature distribution was determined using interaction modeling of selected materials with the laser beam. An effective technique was employed to simulate the temperature changes of the metal and water domains over time and different distances, based primarily on the laser energy changes. This physical model provided insights into the complex interplay between the laser, the metal film, and the surrounding liquid, enabling the optimization of the single-cell sorting process.

**Sequencing**

The 3 μl buffer D2, prepared according to the REPLI-g Single cell kit (Qiagen), was placed in the single-cell receiving tube. Immediately after sorting, microbial cells were ruptured with three freeze-thaw cycles using liquid nitrogen. The sample was then incubated at 65 °C for 10 min, and 0.6 μl of neutralization buffer (supplied in the REPLI-g Single cell kit) was added. The reaction was supplemented with Phi29 DNA polymerase buffer (Qiagen) on ice to amplify the gDNA released from the lysed single cells. The amplified reaction was conducted at 30 °C for 12 hours, followed by denaturation of Phi29 DNA polymerase at 65 °C for 10 min. The gDNA products obtained from a single bacterial cell were stored at −80 °C for subsequent sequencing and analysis. The gDNA products were chosen for library construction and sequenced on the Illumina HiSeq/Nova platform (Azenta Life Sciences). The amplification coverage of the single-cell genome was analyzed.

**Image Processing and Statistical Analysis**

Fluorescence microscopy images were visualized and processed using ImageJ (National Institutes of Health, USA). All data in the study were analyzed using OriginPro 2023 (OriginLab Corporation, Northampton, MA, USA).

## ASSOCIATED CONTENT

### Supporting Information

Additional details. Figure S1 showing design and setup of a Nanowell-LIFT system; Figure S2 showing characterization of the N-chip; Figure S3 showing microscopic images of nanowell array films with different pore sizes; Figure S4 showing fluorescence images of single-cell

capture; Figure S5 showing finite-element analysis of Gaussian and time distribution functions; Figure S6 showing temperature simulations comparing the single-cell sorting performance of the conventional LIFT and the Nanowell-LIFT platforms; Figure S7 showing results of sequence alignments of the single-cell clones cultured after sorting; descriptions for Movie S1 and Movie S2 (PDF).

Movie S1 showing accurate and efficient single-cell sorting of *S. cerevisiae* cells using the Nanowell-LIFT system, taken with bright-field imaging (MP4).

Movie S2 showing single-cell sorting of *S. cerevisiae* cells using the conventional LIFT system, taken with bright-field imaging (MP4).

**ACKNOWLEDGMENTS**

The authors are grateful for the support from the National Natural Science Foundation of China (Grant No. 62104227). The authors also thank the Peking University National Key Laboratory of Science and Technology technicians on micro/nano fabrication for helping with the processes.

**Author Contributions**

Y.W., W.H., and B.L. conceived the original idea. Y.W. and B.L. designed the methodology and the experiments. Y.W. fabricated the devices, conducted simulations, performed the experiments, and analyzed data. H.P. and L.S. simulated optical systems. X.H. completed the automated procedure. P.L., Y.W., F.C., and K.L. tested devices. Y.X. and H.L. conducted guidance for biological experiments. Y.W., Q.X., and W.W. participated in chip design and fabrication. Y.W., Y.X., Y.W., C.Z., and H.Y. analyzed the results. Y.W. wrote the manuscript. B.L. and W.H. supervised the project. B.L. and H.W. provided funds to support the project. All authors edited the manuscript.

**Notes**

The authors declare no competing financial interest.

## REFERENCES


1. Altschuler, S. J.; Wu, L. F. Cellular Heterogeneity: Do Differences Make a Difference? *Cell*. **2010**, *141*, 559-563.
2. Guo, F.; Li, L.; Li, J.; Wu, X.; Hu, B.; Zhu, P.; Wen, L.; Tang, F. Single-Cell Multi-Omics Sequencing of Mouse Early Embryos and Embryonic Stem Cells. *Cell Res.* **2017**, *27*, 967-988.
3. Alemany, A.; Florescu, M.; Baron, C. S.; Peterson-Maduro, J.; Van Oudenaarden, A. Whole-Organism Clone Tracing Using Single-Cell Sequencing. *Nature*. **2018**, *556*, 108-112.
4. Roth, A.; McPherson, A.; Laks, E.; Biele, J.; Yap, D.; Wan, A.; Smith, M. A.; Nielsen, C. B.; McAlpine, J. N.; Aparicio, S. Clonal Genotype and Population Structure Inference from Single-Cell Tumor Sequencing. *Nat. Meth.* **2016**, *13*, 573-576.
5. Casasent, A. K.; Schalck, A.; Gao, R.; Sei, E.; Long, A.; Pangburn, W.; Casasent, T.; Meric-Bernstam, F.; Edgerton, M. E.; Navin, N. E. Multiclonal Invasion in Breast Tumors Identified by Topographic Single Cell Sequencing. *Cell*. **2018**, *172*, 205-217.
6. Kim, C.; Gao, R.; Sei, E.; Brandt, R.; Hartman, J.; Hatschek, T.; Crosetto, N.; Foukakis, T.; Navin, N. E. Chemoresistance Evolution in Triple-Negative Breast Cancer Delineated by Single-Cell Sequencing. *Cell*. **2018**, *173*, 879-893.
7. Keller, M.; Zengler, K. Tapping into Microbial Diversity. *Nat. Rev. Microbiol.* **2004**, *2*, 141-150.
8. Achtman, M.; Wagner, M. Microbial Diversity and the Genetic Nature of Microbial Species. *Nat. Rev. Microbiol.* **2008**, *6*, 431-440.
9. Pike, L. J.; Viciani, E.; Kumar, N. Genome Watch: Microbial Diversity Knows No Borders. *Nat. Rev. Microbiol.* **2018**, *16*, 66-66.
10. Keller, L.; Pantel, K. Unravelling Tumour Heterogeneity by Single-Cell Profiling of Circulating Tumour Cells. *Nat. Rev. Cancer*. **2019**, *19*, 553-567.
11. Ramsköld, D.; Luo, S.; Wang, Y.-C.; Li, R.; Deng, Q.; Faridani, O. R.; Daniels, G. A.; Khrebtukova, I.; Loring, J. F.; Laurent, L. C. Full-Length Mrna-Seq from Single-Cell Levels of Rna and Individual Circulating Tumor Cells. *Nat. Biotechnol.* **2012**, *30*, 777-782.
12. Liu, X.; Chen, B.; Huang, Z.; Duan, R.; Li, H.; Xie, L.; Wang, R.; Li, Z.; Gao, Y.; Zheng, Y. Effects of Poor Sleep on the Immune Cell Landscape as Assessed by Single-Cell Analysis. *Commun. Biol.* **2021**, *4*, 1325.
13. Wu, X.; Liu, Y.; Jin, S.; Wang, M.; Jiao, Y.; Yang, B.; Lu, X.; Ji, X.; Fei, Y.; Yang, H. Single-Cell Sequencing of Immune Cells from Anticitrullinated Peptide Antibody Positive and Negative Rheumatoid Arthritis. *Nat. Commun.* **2021**, *12*, 4977.
14. Berry, D.; Stecher, B.; Schintlmeister, A.; Reichert, J.; Brugiroux, S.; Wild, B.; Wanek, W.; Richter, A.; Rauch, I.; Decker, T. Host-Compound Foraging by Intestinal Microbiota Revealed by Single-Cell Stable Isotope Probing. *Proc. Natl. Acad. Sci. U.S.A.* **2013**, *110*, 4720-4725.
15. Chijiiwa, R.; Hosokawa, M.; Kogawa, M.; Nishikawa, Y.; Ide, K.; Sakanashi, C.; Takahashi, K.; Takeyama, H. Single-Cell Genomics of Uncultured Bacteria Reveals Dietary Fiber Responders in the Mouse Gut Microbiota. *Microbiome*. **2020**, *8*, 1-14.
16. Hatzenpichler, R.; Krukenberg, V.; Spietz, R. L.; Jay, Z. J. Next-Generation Physiology Approaches to Study Microbiome Function at Single Cell Level. *Nat. Rev. Microbiol.* **2020**, *18*, 241-256.

17. Herzenberg, L. A.; Parks, D.; Sahaf, B.; Perez, O.; Roederer, M.; Herzenberg, L. A. The History and Future of the Fluorescence Activated Cell Sorter and Flow Cytometry: A View from Stanford. *Clin. Chem.* **2002**, *48*, 1819-1827.
18. Miltenyi, S.; Müller, W.; Weichel, W.; Radbruch, A. High Gradient Magnetic Cell Separation with Macs. *Cytom. Part A*. **1990**, *11*, 231-238.
19. Schmitz, B.; Radbruch, A.; Kümmel, T.; Wickenhauser, C.; Korb, H.; Hansmann, M.; Thiele, J.; Fischer, R. Magnetic Activated Cell Sorting (Macs)—a New Immunomagnetic Method for Megakaryocytic Cell Isolation: Comparison of Different Separation Techniques. *Eur. J. Haematol.* **1994**, *52*, 267-275.
20. Espina, V.; Heiby, M.; Pierobon, M.; Liotta, L. A. Laser Capture Microdissection Technology. *Expert Rev. Mol. Diagn.* **2007**, *7*, 647-657.
21. Emmert-Buck, M. R.; Bonner, R. F.; Smith, P. D.; Chuaqui, R. F.; Zhuang, Z.; Goldstein, S. R.; Weiss, R. A.; Liotta, L. A. Laser Capture Microdissection. *Science*. **1996**, *274*, 998-1001.
22. Zhong, M.-C.; Wei, X.-B.; Zhou, J.-H.; Wang, Z.-Q.; Li, Y.-M. Trapping Red Blood Cells in Living Animals Using Optical Tweezers. *Nat. Commun.* **2013**, *4*, 1768.
23. Johansen, P. L.; Fenaroli, F.; Evensen, L.; Griffiths, G.; Koster, G. Optical Micromanipulation of Nanoparticles and Cells inside Living Zebrafish. *Nat. Commun.* **2016**, *7*, 10974.
24. Hibi, T.; Dosch, H. M. Limiting Dilution Analysis of the B Cell Compartment in Human Bone Marrow. *Eur. J. Immunol.* **1986**, *16*, 139-145.
25. Sutherland, H. J.; Lansdorp, P. M.; Henkelman, D. H.; Eaves, A. C.; Eaves, C. J. Functional Characterization of Individual Human Hematopoietic Stem Cells Cultured at Limiting Dilution on Supportive Marrow Stromal Layers. *Proc. Natl. Acad. Sci. U.S.A.* **1990**, *87*, 3584-3588.
26. Hempel, C. M.; Sugino, K.; Nelson, S. B. A Manual Method for the Purification of Fluorescently Labeled Neurons from the Mammalian Brain. *Nat. Protoc.* **2007**, *2*, 2924-2929.
27. Guo, Q.; Su, X.; Zhang, X.; Shao, M.; Yu, H.; Li, D. A Review on Acoustic Droplet Ejection Technology and System. *Soft Matter*. **2021**, *17*, 3010-3021.
28. Jentsch, S.; Nasehi, R.; Kuckelkorn, C.; Gundert, B.; Aveic, S.; Fischer, H. Multiscale 3D Bioprinting by Nozzle‐Free Acoustic Droplet Ejection. *Small Methods*. **2021**, *5*, 2000971.
29. Song, Y.; Kaster, A. K.; Vollmers, J.; Song, Y.; Davison, P. A.; Frentrup, M.; Preston, G. M.; Thompson, I. P.; Murrell, J. C.; Yin, H. Single‐Cell Genomics Based on Raman Sorting Reveals Novel Carotenoid‐Containing Bacteria in the Red Sea. *Microb. Biotechnol.* **2017**, *10*, 125-137.
30. Jing, X.; Gou, H.; Gong, Y.; Su, X.; Xu, L.; Ji, Y.; Song, Y.; Thompson, I. P.; Xu, J.; Huang, W. E. Raman‐Activated Cell Sorting and Metagenomic Sequencing Revealing Carbon‐Fixing Bacteria in the Ocean. *Environ. Microbiol.* **2018**, *20*, 2241-2255.
31. Gao, J.; Sun, D.; Li, B.; Yang, C.; Wang, W. Integrated Identification of Growth Pattern and Taxon of Bacterium in Gut Microbiota Via Confocal Fluorescence Imaging‐Oriented Single‐Cell Sequencing. *mLife*. **2022**, *1*, 350-358.
32. Li, H.-Z.; Yang, K.; Liao, H.; Lassen, S. B.; Su, J.-Q.; Zhang, X.; Cui, L.; Zhu, Y.-G. Active Antibiotic Resistome in Soils Unraveled by Single-Cell Isotope Probing and Targeted Metagenomics. *Proc. Natl. Acad. Sci. U.S.A.* **2022**, *119*, e2201473119.
33. Koch, L.; Deiwick, A.; Franke, A.; Schwanke, K.; Haverich, A.; Zweigerdt, R.; Chichkov,

B. Laser Bioprinting of Human Induced Pluripotent Stem Cells—the Effect of Printing and Biomaterials on Cell Survival, Pluripotency, and Differentiation. *Biofabrication*. **2018**, *10*, 035005.

34. Wang, Y.; Xu, J.; Cui, D.; Kong, L.; Chen, S.; Xie, W.; Zhang, C. Classification and Identification of Archaea Using Single-Cell Raman Ejection and Artificial Intelligence: Implications for Investigating Uncultivated Microorganisms. *Anal. Chem.* **2021**, *93*, 17012-17019.

35. Zhao, X.; Meng, X.; Liu, Y.; Bai, S.; Li, B.; Li, H.; Hou, N.; Li, C. Single-Cell Sorting of Microalgae and Identification of Optimal Conditions by Using Response Surface Methodology Coupled with Life-Cycle Approaches. *Sci. Total Environ.* **2022**, *832*, 155061.

36. Koch, L.; Deiwick, A.; Chichkov, B. Laser-Based 3D Cell Printing for Tissue Engineering. *BioNanoMaterials*. **2014**, *15*, 71-78.

37. Delrot, P.; Hauser, S. P.; Krizek, J.; Moser, C. Depth-Controlled Laser-Induced Jet Injection for Direct Three-Dimensional Liquid Delivery. *Appl. Phys. A*. **2018**, *124*, 1-8.

38. Wang, Y.; Ji, Y.; Wharfe, E. S.; Meadows, R. S.; March, P.; Goodacre, R.; Xu, J.; Huang, W. E. Raman Activated Cell Ejection for Isolation of Single Cells. *Anal. Chem.* **2013**, *85*, 10697-10701.

39. Gan, C.; Wu, R.; Luo, Y.; Song, J.; Luo, D.; Li, B.; Yang, Y.; Xu, M. Visualizing and Isolating Iron-Reducing Microorganisms at the Single-Cell Level. *Appl. Environ. Microbiol.* **2021**, *87*, e02192-02120.

40. Liang, P.; Liu, B.; Wang, Y.; Liu, K.; Zhao, Y.; Huang, W. E.; Li, B. Isolation and Culture of Single Microbial Cells by Laser Ejection Sorting Technology. *Appl. Environ. Microbiol.* **2022**, *88*, e01165-01121.

41. Chang, T. Y.; Yadav, V. G.; De Leo, S.; Mohedas, A.; Rajalingam, B.; Chen, C.-L.; Selvarasah, S.; Dokmeci, M. R.; Khademhosseini, A. Cell and Protein Compatibility of Parylene-C Surfaces. *Langmuir*. **2007**, *23*, 11718-11725.

42. Song, Y.; Cui, L.; López, J. Á. S.; Xu, J.; Zhu, Y.-G.; Thompson, I. P.; Huang, W. E. Raman-Deuterium Isotope Probing for *in-situ* Identification of Antimicrobial Resistant Bacteria in Thames River. *Scientific reports*. **2017**, *7*, 1-10.

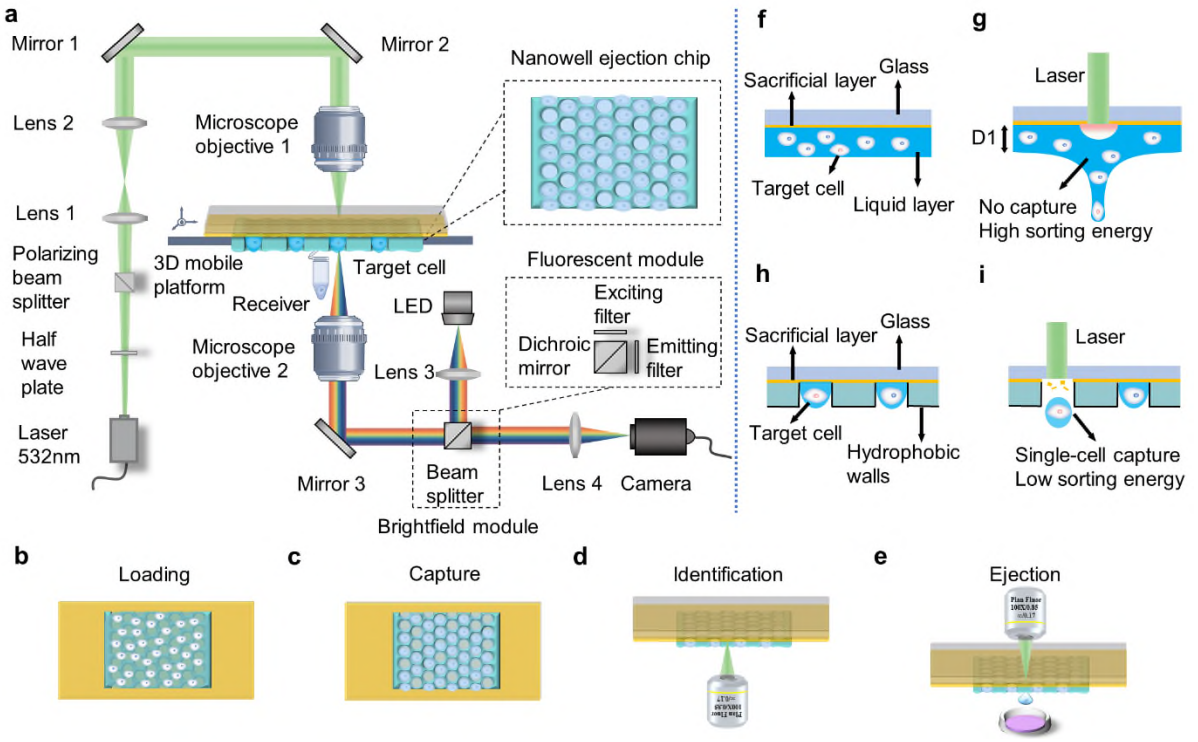


**Figure 1**. Design and operating principle of the Nanowell-LIFT platform. (a) Schematic diagram of the Nanowell-LIFT platform. The device consists of a 532 nm pulsed laser, a half-waveplate, a polarizing beam splitter, four lenses, three mirrors, two microscopy objectives, a beam splitter (a dichroic mirror, an exciting filter, and an emitting filter), a LED, a camera, a 3D mobile platform, a receiver, and an N-chip. (b-e) Schematic representation of single-cell sorting process setup. (f-g) Schematic diagrams of conventional LIFT sorting models, with D1 representing layer thickness. (h-i) Schematic diagrams of Nanowell-LIFT sorting models.

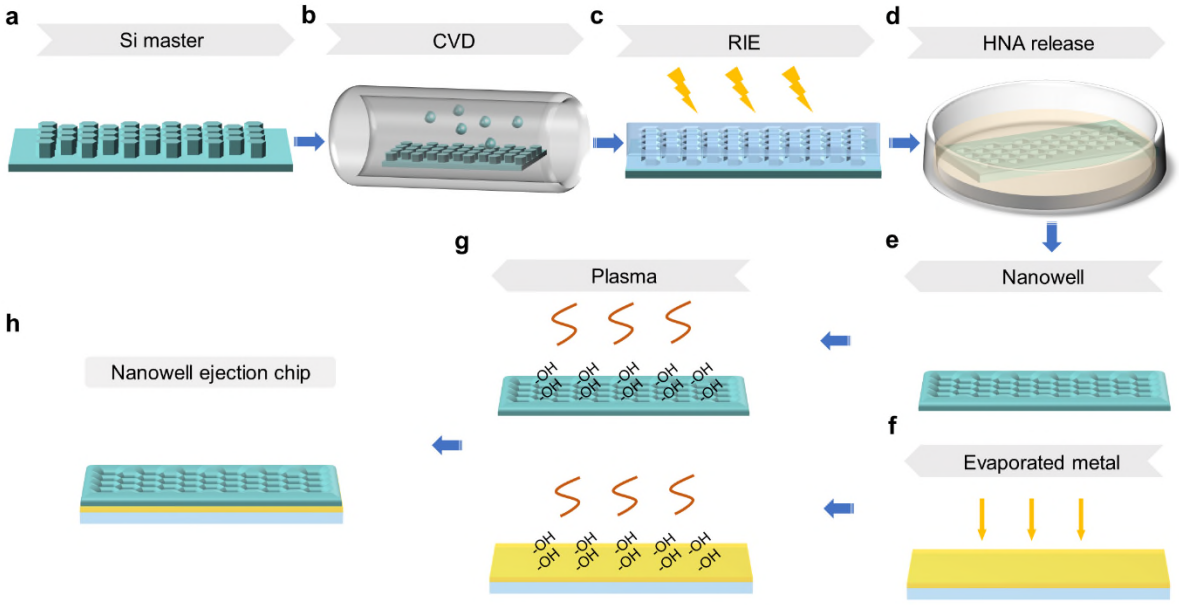


**Figure 2.** Precise fabrication and pre-treatment of the N-chip. (a) Fabrication of silicon master by photoresist lithography. (b) Chemical vapor deposition (CVD) of Parylene C onto the silicon master. (c) Reactive ion etching (RIE) of redundant Parylene C. (d) Release of the nanowell films by HNA etching. (e) Acquisition of hydrophobic nanowell films. (f) Evaporation of metal on a glass substrate. (g) Plasma treatment on both the metal surface and the nanowell surface. (h) Assembly of the N-chip.

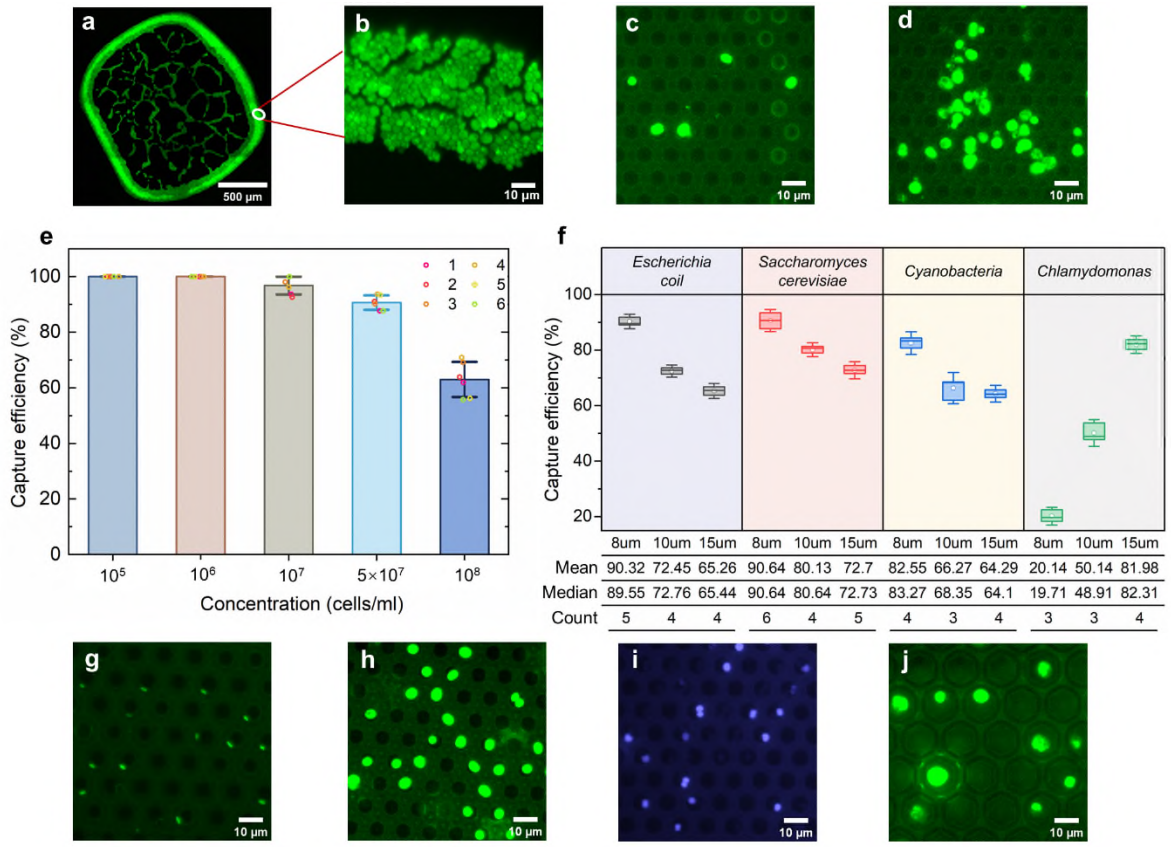


**Figure 3.** Characterization of the N-chips for single-cell capture. (a) Fluorescence image of the *S. cerevisiae* cells distributed on a conventional metal-coated ejection chip. Scale bars, 500 μm. (b) Magnified fluorescence image of (a). Scale bars, 10 μm. (c, d, h) Fluorescence images of the *S. cerevisiae* cells captured on an N-chip at cell suspension concentrations of $10^7$ cells/ml, $10^8$ cells/ml, and $5\times10^7$ cells/ml, respectively. Scale bars, 10 μm. (e) Single-cell capture efficiency of the *S. cerevisiae* cells captured at different cell concentrations. (f) Single-cell capture efficiency of various cell lines captured at different nanowell pore sizes. (g-j) Fluorescence images of various cell lines captured at the optimal pore size under a suspension concentration of $5\times10^7$ cells/ml. Scale bars, 10 μm.

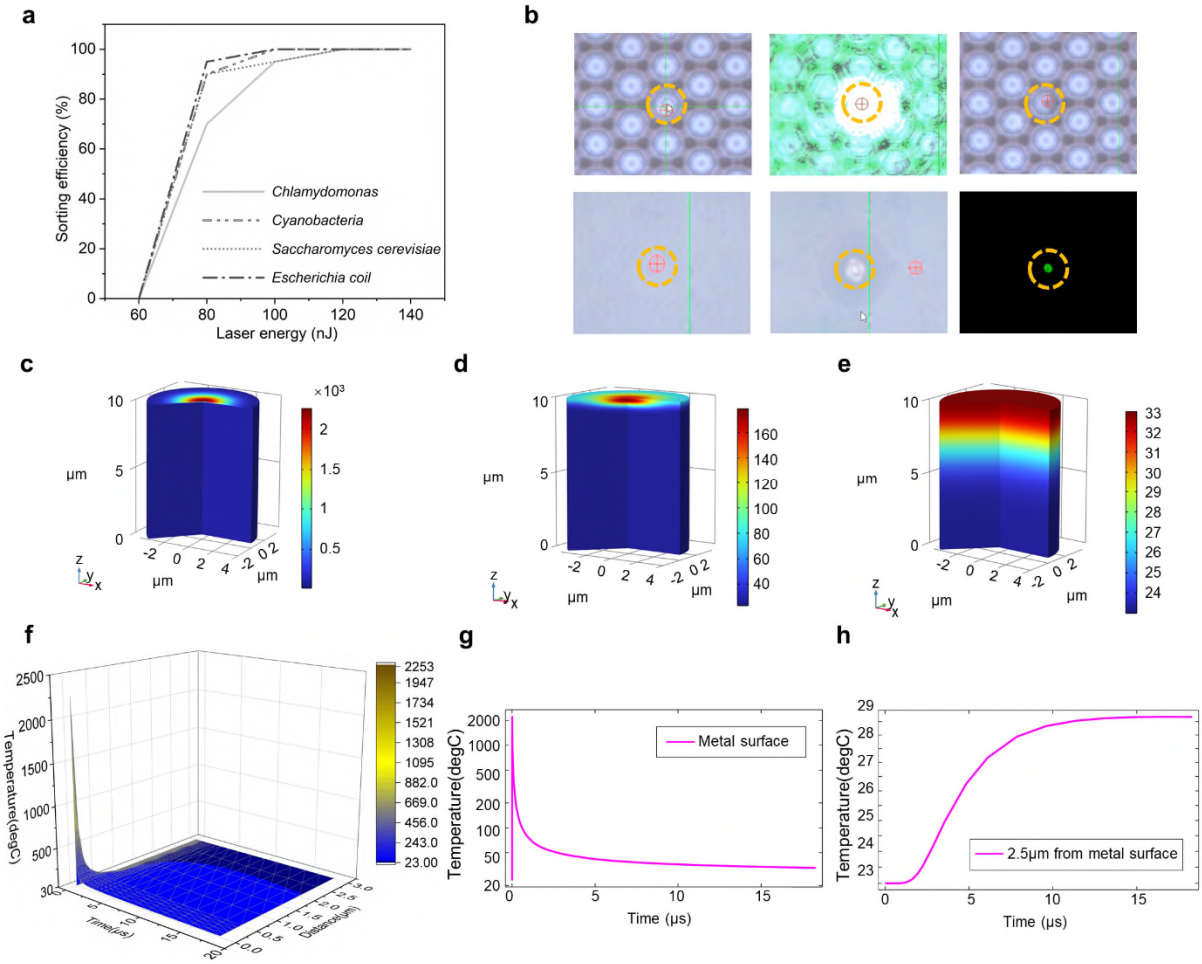


546

547 **Figure 4**. Performance and temperature simulation of single-cell sorting for the Nanowell-LIFT
548 system. (a) Evaluation of single-cell sorting efficiency for various cell lines by adjusting the
549 laser energy. (b) Dynamic process of single *S. cerevisiae* cell sorting based on the Nanowell-
550 LIFT platform. (c) Temperature distribution model of the nanowell liquid environment at 9 ns
551 after laser ablation of the sacrificial layer. (d) Temperature distribution model of the nanowell
552 liquid environment during sorting at 500 ns. (e) Temperature model of the nanowell liquid
553 environment at 17 μs after sorting. (f) The temperature changes are related to the vertical
554 distance and time of the laser action. The Royal Blue zone represents a temperature range of
555 23-30 degrees Celsius. (g) Temperature variation of the sacrificial layer surface after laser
556 ejection over time. (h) Temperature variation of the position of 2.5 μm from the sacrificial layer
557 surface after laser ejection over time.

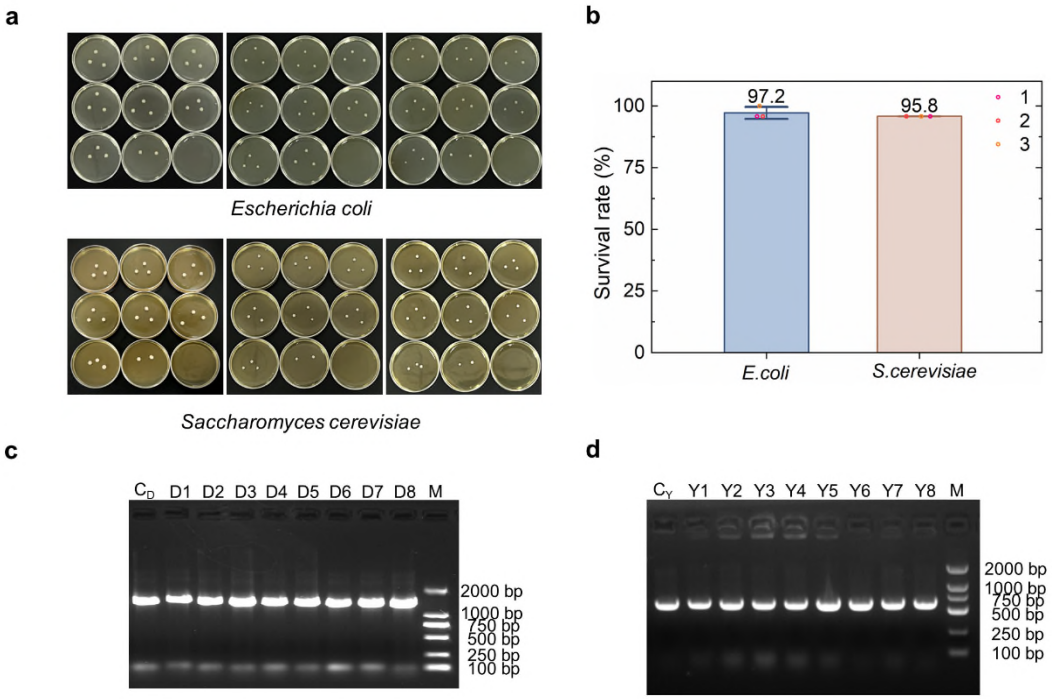


**Figure 5.** Verification of cell viability on cell sorting performance. (a) Photographs of *E. coli* and *S. cerevisiae* cells after single-cell sorting and incubation for 36 hours. (b) The survival rate of sorted single cells after 36 hours of incubation. (c) Photograph of gel electrophoresis from control *E. coli* cell suspension ($C_D$) and single-cell colonies for *E. coli* (D1-D8). M, DNA ladder. (d) Photograph of gel electrophoresis from control *S. cerevisiae* cell suspension ($C_Y$) and single-cell colonies for *S. cerevisiae* (Y1–Y8). M, DNA ladder.

**Table 1.** Data statistics of the functional single-cell genome coverage of samples *E. coli* by Nanowell-LIFT and traditional LIFT.

| **Sample** | ***E. coli* with Nanowell-LIFT** | ***E. coli* with Traditional LIFT** |
|---|---|---|
| Genome Bases (bp) | 4641652 | 4641652 |
| Covered Bases (bp) | 4087280 | 1785274 |
| GC% | 49.50 | 48.36 |
| Coverage (%) | 88.06 | 38.46 |